IPPI
Polyolefins Journal Vol. 10, No. 1 (2023)
DOI: 10.22063/POJ.2022.3221.1232
ORIGINAL PAPER

Polyvinylpyrrolidone and polystyrene composites based on economical high quality biofillers derived from rice husk: Spectroscopic and hydrophilic investigations

Hamed Nazarpour-Fard

Department of Chemistry, Faculty of Sciences, Lorestan University, Khorramabad, Iran

Received: 24 August 2022, Accepted: 28 October 2022

ABSTRACT

Polyvinylpyrrolidone (PVP) composites based on rice husk (RH), rice husk carbon (RHC, i.e., black rice husk ash (BRHA)) and rice husk ash (RHA, i.e., white rice husk ash (WRHA)) were prepared separately through solution casting method. Similar composites were made using polystyrene (PS) through the same protocol. The carbon and ash obtained from this type of rice husk were obtained via pyrolysis at 300 and 600°C, respectively, for 1 hour. The effects of these additives on the spectroscopic characteristics of polymers were verified by examining the infrared (FT-IR) and X-ray diffraction (XRD) spectra of the prepared composites. The resulting showed a remarkable difference between the spectra of parent polymers and the corresponding composites. Changes in peak width and 2θ parameters (observed in XRD patterns) revealed that PVP possesses better interactions with RHC, while PS has better interactions with RHA. Due to the high hydrophilicity of PVP, some investigations were accomplished on the hydrophilic properties of PVP samples. Polystyrene did not reveal detectable water vapor absorption (WVA), thus this experiment was not carried out for PS samples. Eventually, it was disclosed that there are significant discrepancies between the hydrophilic properties of PVP and its composites. In the other word, the WVA decreased from 290% for parent PVP to 210% for PVP-RHC composite. **Polyolefins J (2023) 10: 45-57**

Keywords: Polyvinylpyrrolidone; polystyrene; rice husk derivatives; bio-composite; spectroscopic and hydrophilic characteristics.

INTRODUCTION

Nowadays, rotational molding is taken into consideration Preparation of composites as multi-phase and multi-component materials is a versatile and applicable method to improve material properties, including thermal [1,2], mechanical [3,4,5], electrical [6,7-9], barrier [10], and many other characteristics of polymers.

In addition to the methods of melt mixing, electrospinning and in-situ polymerization, solution casting is also one of the most common and simple methods for preparing polymeric composites. In this procedure, the well-distributed solution of additives in polymer is subjected to solvent evaporation at the suitable temperature for the fabrication of the desired composite. For example, this method was employed to prepare the composites of polyvinyl alcohol/polyethylene oxide/LiOH [11], poly-methylmethacrylate/nanographite [12], starch/kaolin/

*Corresponding Author - E-mail: Nazarpour.ha@lu.ac.ir; Nazapoorfard@gmail.com

cellulose fibers of rice husk [13], polyvinylidene fluoride /reduced graphene oxide [14], polymethyl methacrylate/graphene oxide [15], and polyhydroxybutyrate/ cellulose/calcium carbonate [16].

Polyvinylpyrrolidone is soluble in water and biological fluids, which is known as a non-toxic and non-digestible substance. Therefore, it is widely used in many pharmaceutical and medical applications. As hydrophobic PVP composites have been studied in Ref. [50], for the application of PVP in some medical purposes, it is sometimes necessary to reduce the hydrophilicity of this polymer. As a result, PVP is widely used to provide composites [17], nanocomposites [18], bio-composites [19] and in the structure of many catalysts with interesting performance [20]. In another research study, chitosan/PVP composites were studied as hemostatic materials for using in blood coagulation and hemostasis applications, which their hydrophilicity is an important issue [21].

Polystyrene is an important general purpose polyolefin employed in numerous industrial and research applications, among these, we can mention PS composites with their amazing applications. Investigation of the electrical, mechanical, and biological characteristics of polystyrene composites has been the subject of many articles [22-24]. Ighalo et al. investigated the thermal behavior, microstructural characteristics and moisture absorption of rice husk waste-incorporated PS composites [25].

Incorporation of biomaterials, for example, abundantly available plant wastes, into polymer matrices has attracted increasing attention. This prevents the excessive consumption of non-renewable resources and leads to environmental conservation. Natural filler/polymer bio-composites have revealed multiple advantages of renewability, low cost and density, chemical modification ability, biodegradability and non-toxicity. These bio-composites have been found to possess the potential to be used in different fields such as structural utilizations [26-28]. For example, ash materials originating from natural wastes such as rice husk ash have been used as cost-effective fillers as well as in various catalytic systems. RH is an agricultural waste, which is abundantly produced in the rice-related industries. Making composites from this biofiller is an important way to use agricultural waste without visible environmental problems. [29]. Rice husk [30], its derivatives [31] and its composites [32] have been successfully employed to remove contaminations from various solutions as well as to amend water absorption and curing behavior of concrete [33]. Also, rice hull has been used for reinforcing polyolefins such as polypropylene and polyethylene [34]. The above explanations show the importance of using biological materials in protecting the environment. Thus, the rice husk and its carbon and ash derivatives were used as bio-additives to improve the spectroscopic characteristics (FT-IR and X-ray diffraction spectra) of PVP and PS. These additives also changed the hydrophilicity of polyvinylpyrrolidone.

EXPERIMENTAL

Materials

Polyvinylpyrrolidone (type K30) was purchased from Sobhan Pharmaceutical Company (Rasht, Iran). The rice husk employed in this research work and its preparation protocol were the same as ones reported in Ref. [35]. Also, the simple pyrolysis of the prepared rice husk sample in a lab-scale furnace led to the rice husk ash as formerly reported [35]. Polystyrene was synthesized by suspension polymerization method based on the published article [36]. Toluene that was used as the proper solvent for dissolving polystyrene to prepare the PS composites, was produced by Merck Chemical Company.

Methods

Instrumentation

The sonication dispersion of the additives in the solutions was done using an ultrasonic bath, Sono Swiss, Sw3H, Switzerland. Knauer Instrument (Germany) was employed for recording the gel permeation chromatography (GPC) spectrums to evaluate the average molecular weight and polydispersity index of the prepared polystyrene. X-ray diffraction (XRD) measurements were accomplished on a Philips diffractometer of PW1840 (made in Netherlands) with Cu-Kα radiation. Fourier transform infrared (FT-IR) spectra were recorded on a Bruker Alpha FT-IR instrument using KBr disks. Preparing the carbonic and the ash materials from the

rice husk was accomplished using a Nabertherm furnace (made in Germany) adjustable up to the temperature of 3000°C. The chemical composition of RHA (WRHA) and RHC (BRHA) was examined by using a Philips X-ray fluorescence (XRF) spectrometer (Model Magix Pro).

Synthesis of polystyrene

The polystyrene sample studied in this paper was synthesized from styrene monomer via suspension polymerization. Here, benzoyl peroxide was employed as the convenient initiator for radical polymerization. This process was carried out in a three-necked balloon under nitrogen atmosphere and specific conditions according to the protocol reported by Slobodian et al. [36]. The balloon was equipped with a mechanical stirrer to properly agitate the reaction medium during the polymerization process.

Preparing RH, RHC and RHA

The rice husk (RH) (Figure 1a) was provided using the steps of milling, washing with distilled water, drying, smashing and then sieving by a stainless-steel sieve (200 mesh size), respectively as reported in Ref. [35]. The carbon preparation from this rice husk sample was done by burning the rice husk in the furnace under the constant temperature of 300ºC for 1 hour (see Figure 1b). The rice husk ash (Figure 1c) was fabricated by the pyrolysis of the finely powdered rice husk at the elevated temperature (600ºC) for 1 hour as the reported protocol [35].

Preparation of the composites

A certain amount (0.002 g) of the desired additive was poured into the aqueous solution containing 0.1 g of PVP which was simultaneously stirred by a magnetic stirrer. The resulting mixture was subjected under agitation using a magnetic stirrer for 24 hours at ambient temperature. Then, for the better dispersion of the additive particles, the relevant solution was exposed to ultrasonic waves by an ultrasonic bath. At the end, the uniformly distributed additive in the PVP aqueous solution, was poured on a glass plate and completely dried using oven heating at the temperature of 60ºC. Finally, the presented composites were kept in suitable conditions for use in various tests.

Measurement of water vapor absorption of the samples

In order to check the hydrophilic traits of the polyvinylpyrrolidone samples, two simple procedures were employed. In the first method, 0.01 g of each sample was carefully weighed and placed on a filter paper with a given weight. Then, it was placed in a closed WVA chamber for 24 hours at ambient temperature and pressure. During the WVA tests, the chamber contained 2 mL water and possessed the same dimensions as presented in Figure 2. After the absorption of water vapor by the PVP samples from the atmosphere of the chamber, the samples were taken out. The differences

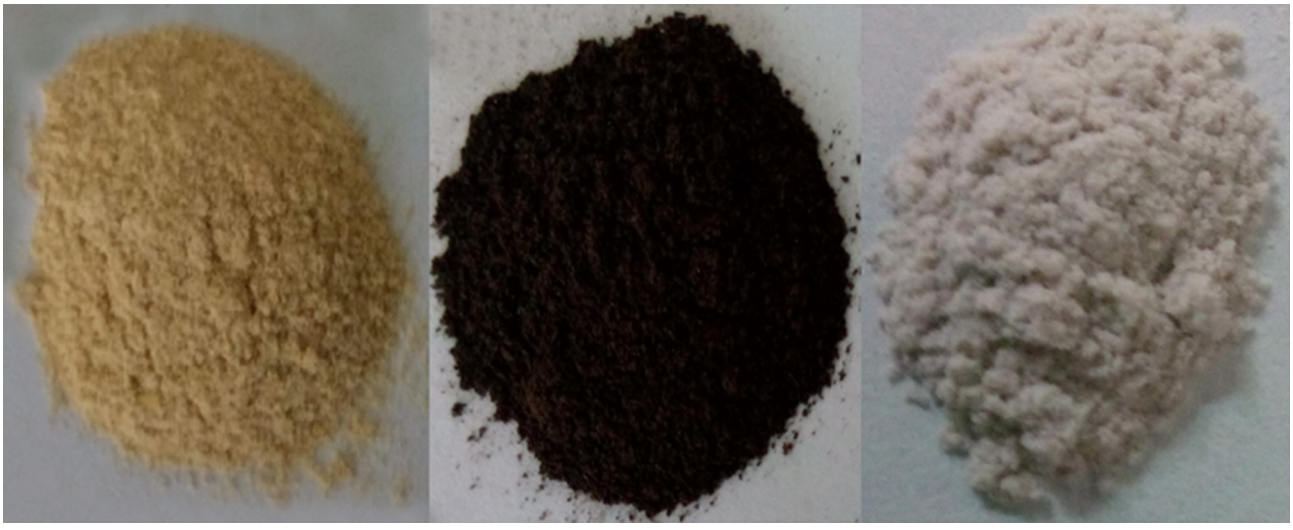

(a) (b) (c)

Figure 1. Images of bio-additives: (a) rice husk, (b) rice husk carbon and (c) rice husk ash.

between the initial and final weights of the samples were considered as the sign of their water vapor absorption. It should be noted that the WVA% values of PVP and the composites were computed using equation 1.

$$\text{WVA (\%)} = \frac{\text{initial weight - final weight}}{\text{initial weight}} \times 100 \qquad (1)$$

In the second way, the same amount of each sample was placed on filter paper and incubated for 24 hours in the same chamber and conditions. After leaving the sample from the chamber, the wetted paper area due to water absorption by the sample was qualitatively described (Figure 7). Then, the area of this circular area was compared for pure PVP and composites. This protocol was a qualitative expression of sample hydrophilic, where larger wetted area means greater WVA and hydrophilicity.

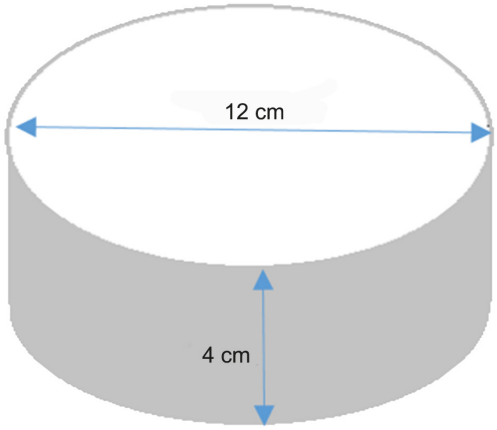

Figure 2. Schematic representation of the chamber dimensions used for WVA tests.

RESULTS AND DISCUSSION

Additives composition

The main components of RH sample were examined using the methods reported in the literature [35,37] and the results are tabulated in Table 1. Also, the prepared RHA was found to contain silica (80.82%) as the main element, which is shown along with other components in Table 1, just like what was reported in the previous study [35,38]. It was observed that the weight loss of RH during pyrolysis is 79.4 ± 1 %. In the other word, RH has a solids content of 20.6 ± 1% because the carbon content is burnt off and almost all that remains is the silica content of RiH [35]. Many parameters affect the characteristics of rice husk ash such as RH composition, pyrolysis temperature, and the time during which RH burning continues. The thermal stability of the RiHA sample was found to be 600ºC as reported in Ref. [39] for the same material. Also, the chemical composition of RHC was consistent with the results presented in Table 1. As can be seen, the LOI quantity of RHC was higher than that of RHA, while its silica content was lower as compared to RHA that can be attributed to the unburned carbon present in RHC (black rice husk ash).

Gel permeation chromatography (GPC)

GPC analysis was employed to describe the molecular weight and the molecular weight distribution (PDI) of the as-prepared polystyrene. The results of gel permeation chromatography are exhibited in Table 2. As seen from these data, PS was found to possess the weight and number average molecular weight values

Table 1. The content of the main components in the bio-additives.

RHA (WRHA) components (wt.%)		RHC (BRHA) components (wt.%)		RH Components (wt.%)	
Al_2O_3	0.25	Al_2O_3	1.2	Cellulose	27.4
LOI	12.70	LOI	38.1	Volatile	8.2 ± 0.3
K_2O	1.25	K_2O	5.7	Moisture	5
SiO_2	80.82	SiO_2	40	Silica	14.2
Fe_2O_3	0.38	Fe_2O_3	1.4	Hemicelluloses	18.3
P_2O_5	0.44	P_2O_5	1.7	Lignin	25.8
SO_3	0.39	SO_3	2.1	Inorganics	5.8
Cl	1.99	Cl	4	Soluble	3.5
CaO	0.82	CaO	4.5		
Na_2O	0.96	Na_2O	1.5		

of 33949 and 19905 g mol^{-1}, respectively. The molecular weight distribution for this prepared polymer was similar to that of the commercial polystyrene as presented in the literature [40].

XRD spectroscopy

The degree of crystallinity is considered as one of the most important traits of polymer compounds, which can affect the physical/mechanical properties (e.g., size and shape of the crystallites) of polymeric materials. Scherer's equation is usually used in X-ray diffraction and crystallography studies, which relates the particle/crystal size of the solid substance to the width of XRD peaks. Scherer's equation can be written as follows [41]:

$$\tau = \frac{K\lambda}{\beta \cos\theta} \quad (2)$$

Where τ is the average size of the crystal region and K is the dimensionless shape factor whose value is usually around 0.9 but is proportional to the crystal shape. β is full widths at half maximum (FWHM) of the XRD peaks which is sometimes expressed as Δ(2θ), the parameter θ is Bragg angle, while λ is wavelength of X-ray. A larger FWHM means a smaller size of the crystalline regions (Equation 2). Crystallinity of polymer composites which is considered as a main factor controlling their physical characteristics, can also be checked qualitatively via X-ray diffraction analysis [41]. Crystalline areas in materials are generally appeared as sharp XRD peaks, whereas broad peaks seen in the XRD patterns are attributed to amorphous regions/materials. Therefore, X-ray diffraction is the substantial and multi-purpose procedure for the study of composites.

As can be seen in the XRD patterns (Figure 3), the broad peak at 2θ of 23 is assigned to the parent PVP indicating the disordered structure of this polymer. It is interesting to note that the width of this peak has decreased in the PVP-RiHC composite, which means the crystallinity enhancement (the enhanced crystal size) in comparison to the pure polymer. Probably, the relatively strong interactions between PVP and the additives have been formed. Also, polymer strands have probably oriented in the crystal structures, leading to the structural arrangement, and creation/induction of the new crystallinity in the polymer matrix. Likewise, the appearance of this peak for PVP-RiHC at the lower 2θ values indicates the enhanced crystalline size and the increased d parameter (see equation 3) as compared to those of parent PVP [42]. For more information about this explanation, Ref. [42] could be suitable. These alterations in the crystallinity could be due to the change in intermolecular bonds and molecular order of polyvinylpyrrolidone after incorporating the filler into it.

$$\lambda = 2(\text{d-spacing})\sin\theta \quad (3)$$

In addition, for the composites containing rice husk ash and rice husk, no noticeable changes were observed in the peak width, whereas the 2θ parameter was shifted to the lower values as compared to the neat PVP. It is necessary to mention that the intensities of the peak at 2θ of ~5 in both PVP-RiH and PVP-RiHA have dramatically increased, which reveals the creation of a new type of crystallinity after combining PVP with these additives. In general, all these observations mean that the bio-additives play an effective role on the molecular arrangement and the crystallinity of PVP.

In the spectra of polystyrene samples (Figure 4), the most important observation was the narrowing of the

Table 2. Average molecular weight and PDI data for synthesized polystyrene.

Parameter	Value
Polydispersity Index	1.705
Z Average Molecular Weight	56512 g mol^{-1}
Z+1 Average Molecular Weight	84505 g mol^{-1}
Peak Molecular Weight	22409 g mol^{-1}
Number Average Molecular Weight (M_n)	19905 g mol^{-1}
Weight Average Molecular Weight (M_w)	33949 g mol^{-1}

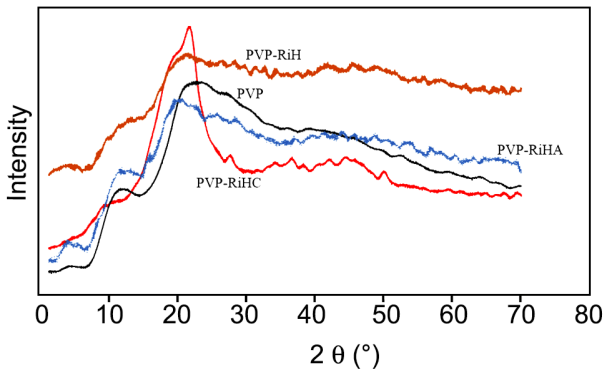

Figure 3. XRD patterns of PVP and its composites.

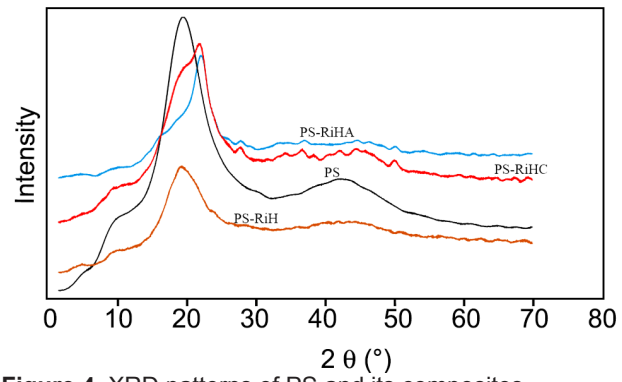

Figure 4. XRD patterns of PS and its composites.

main peak in PS-RHA compared to other samples. This narrowing leads to an increment in the size of crystalline regions. Additionally, the peaks at 2θ around 20 have been shifted to the higher positions for the PS composites in comparison to the parent PS, showing the decreased effect of the additives on the d-spacing parameter. The intensities of polystyrene XRD peaks also decreased after compositing with biomaterials. All these findings demonstrate changes in the molecular order and crystallinity of this polymer through its interactions with bio-originated materials.

From X-ray diffraction spectroscopy, it was concluded that PVP has better interactions with RHC, but PS possesses better interactions with RHA. These differences in polymer/additive interactions can be attributed to mismatches in the chemical nature and rigidity (ability of molecular movements) of these polymers.

FT-IR spectroscopy

From the infrared spectra of the samples (Figures 5 and 6), it is clear that the spectra of pure polymers and their composites are different from each other. In the PS spectra (Figure 5), the bands appearing at the region of 1660-2000 cm^{-1} are attributed to the C-H bending deformations of the benzene ring. The peaks at 1446 and 1490 cm^{-1} are assigned to the stretching-

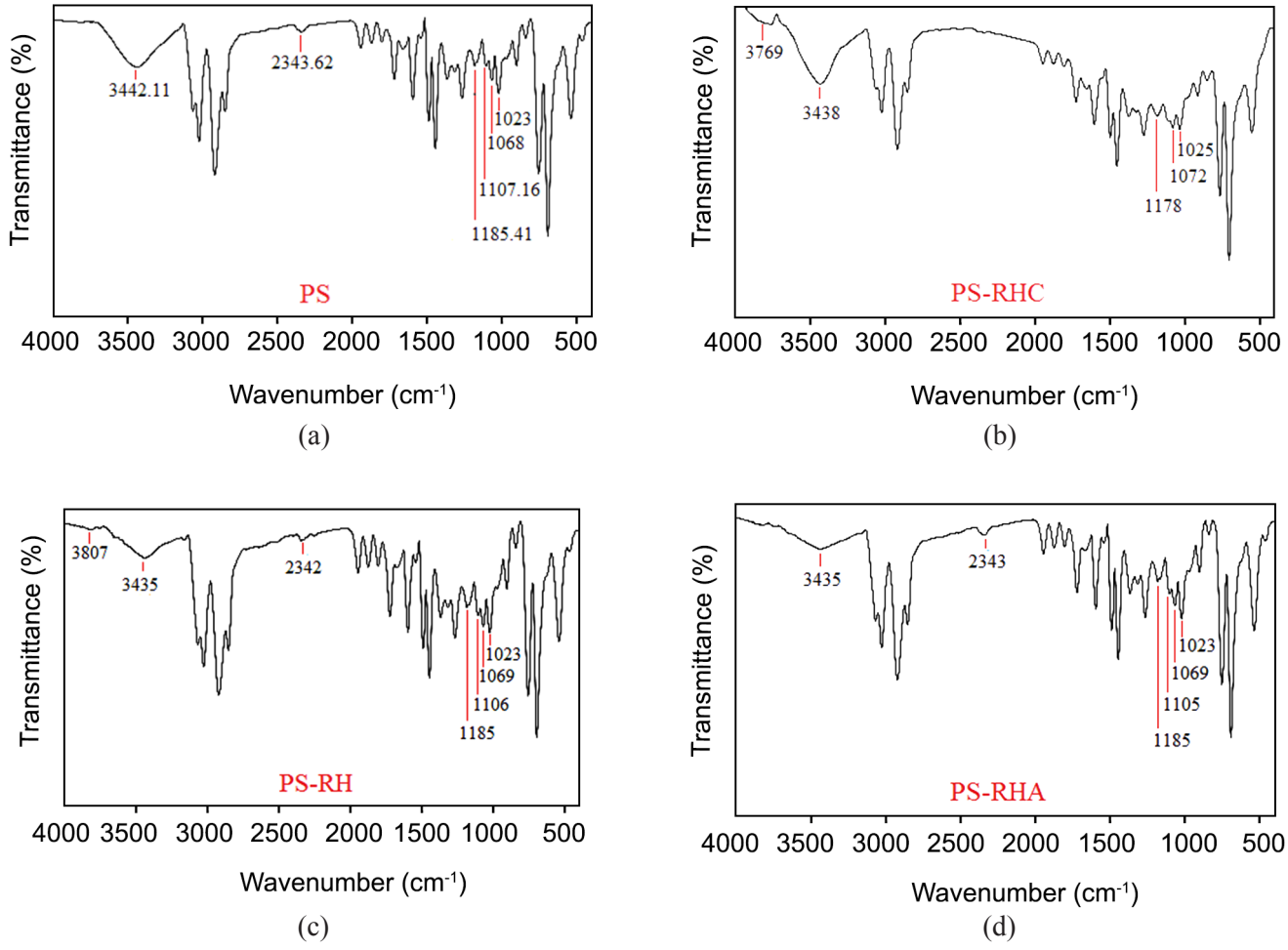

Figure 5. FT-IR spectra of PS and its composites.

vibrational mode of the benzene segment. Moreover, the peaks located at 757 and 695 cm^{-1} could be due to the C-H bending vibration mode of the benzene part of PS [43]. The peaks appeared in the ranges of 2700-3100 cm^{-1} (related to C-H stretching modes of the benzene ring), and 2850-2920 cm^{-1} (attributed to the saturated C-H stretching deformations) were also seen in the FT-IR results as well as the band appeared at 1596 cm^{-1} (assigned to the aromatic C=C bonds) [44]. The peak at 3442 cm^{-1} could be related to the O-H stretching vibrations (due to the presence of very small amounts of absorbed water in the samples) or to the overtone of the peak observed at 1720 cm^{-1}. It should be mentioned that a sharp decrease in the intensity of the peak at 3442 cm^{-1} occurred for PS. Also, it was shifted to wavenumbers of 3438 cm^{-1} for PS/RHC and 3435 cm^{-1} for PS/RH and PS/RHA. These shifts in wavenumber are noticeable and can be due to the interactions occurred between silica (present in the additive) and the functional sites in the polystyrene structure.

Furthermore, the peaks located at 3769 and 3807 cm^{-1} were observed for polystyrene/carbon and polystyrene/rice husk composites, respectively. The peak appeared at 3769 cm^{-1}, which has a high intensity, could be due to the presence of Si-OH and $Si(OH)_2$ surface groups in this composite, as mentioned in Ref [45]. The shift of polystyrene peak from 1185.4 cm^{-1} to 1178 cm^{-1} for PS/RHC sample is another important change in this spectrum. All these drastic changes, i.e., peak shift and peak intensity reduction, are strong reasons for uniform and proper formation of composites.

In the case of polyvinylpyrrolidone (Figure 6), the stretching vibration of C=O bond of the amide functional groups appeared at about 1654 cm^{-1}. The wavenumber of this peak was changed for composites, especially in PVP/RHA, which contains more SiO_2 compared to other composites. This indicates that the O and N atoms of this polymer (which have high electronegativity and non-bonded electron pairs) have formed interactions with bio-additives [32,46-47]. The peaks at 1014, 1222 and 1431 cm^{-1} were attrib-

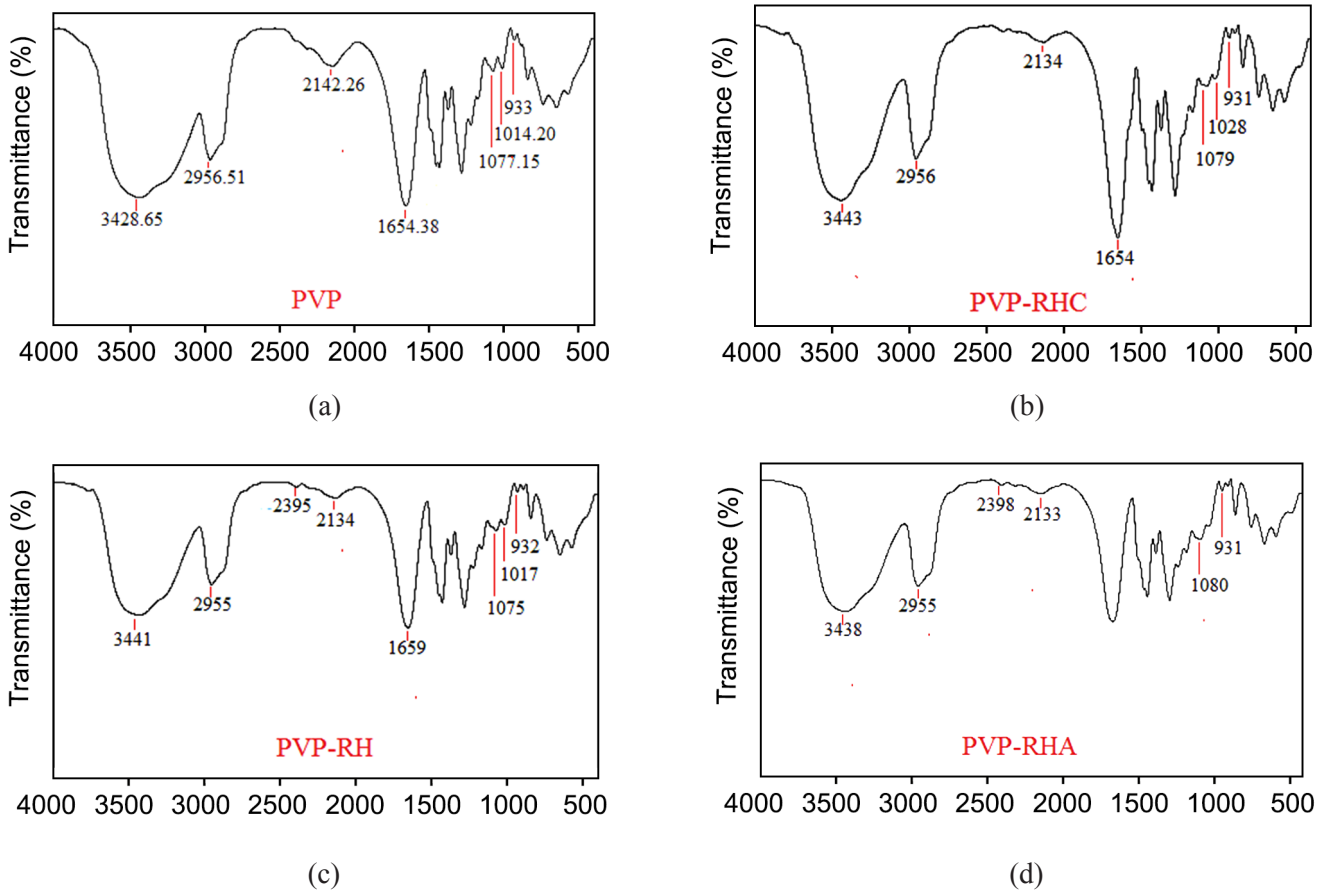

Figure 6. FT-IR spectra of PVP and its composites.

uted to the rocking, twisting and scissoring vibrations of CH_2 [31]. Additionally, the peak appearing at 3428 cm^{-1} was related to the stretching vibration of O-H bond (due to water absorbed on the polymer surface). This peak showed both drastic changes in the wavenumber and decrement in the intensity for the related composites [47]. Also, the peak observed at about 2142 cm^{-1} in the composites was removed, i.e., its intensity was strongly reduced and shifted significantly towards lower wavenumbers. For example, PVP/RHA showed a 10 cm^{-1} reduction in the wavenumber of this peak. The peak appeared at ~1014.2 cm^{-1} was attributed to the stretching vibration of C-N bond as mentioned in Ref [48]. It was shifted to the wavenumber of 1028 cm^{-1} for PVP/RHC and to 1017 cm^{-1} for PVP/RH, while it removed for PVP/RHA. This displacement can be owing to the interactions of N atoms in the PVP structure with natural additives. Generally, all these changes in wavenumbers and intensities of FT-IR peaks after adding these bio-materials indicate the creation of mutual interactions between additives and polymers that are sufficient reasons to demonstrate the proper formation of composites.

Hydrophilicity investigations of PVP and its composites

Polyvinylpyrrolidone is a well-known material due to its very hydrophilic nature and solubility in water. This is why it has been used as a hydrogel material in hydrophilic drugs [49]. When this polymer is in contact with atmosphere, it absorbs water molecules due to its high polarity, thereby, its shape changes from a powdery state to a stacked morphology. The absorbed water acts as a softener and reduces the strength of the PVP samples. During 24 hours exposure of PVP in the laboratory atmosphere, it retained a powdery morphology (its WVA did not change), which could possibly be due to the low amount of water vapor in the laboratory atmosphere. But, the concentration of water vapor in the chamber (Figure 2) was much higher than that of the out of chamber. Thus, the samples immediately absorbed the water vapor during incubation in the chamber and turned into a jelly state after approximately 1 hour. So, the humidity chamber was found to be a suitable system for performing hydrophilicity tests.

Table 3. WVA results for the samples after 24 h of incubation in the humidity chamber.

Sample	Initial weight (g)	Final weight (g)	Absorption (g)	Absorption (wt.%)
PVP	0.01	0.039	0.029	290
PVP-RHA	0.01	0.035	0.025	250
PVP-R	0.01	0.034	0.024	240
PVP-C	0.01	0.031	0.021	210

Although this polymer is soluble in water, reducing its hydrophilicity can be an attractive target for some applications. For example, the amount of WVA obtained from hydrophobic composite drugs containing PVP has been reviewed in Ref [50]. Here, all the polyvinylpyrrolidone composites revealed a lower ability to absorb water compared to pure PVP, the corresponding data are shown in Table 3. In fact, this reduction in hydrophilicity obtained by using environmentally friendly bio-materials could be a beneficial finding for PVP applications where less hydrophilic property is required. As seen in Table 3, Among the composites, PVP-RHC showed significantly higher resistance to water absorption (210% WVA) compared to other samples. A logical explanation for this hydrophilicity decrement can be the relatively strong interactions between PVP and bio-additives. Because, these inter-

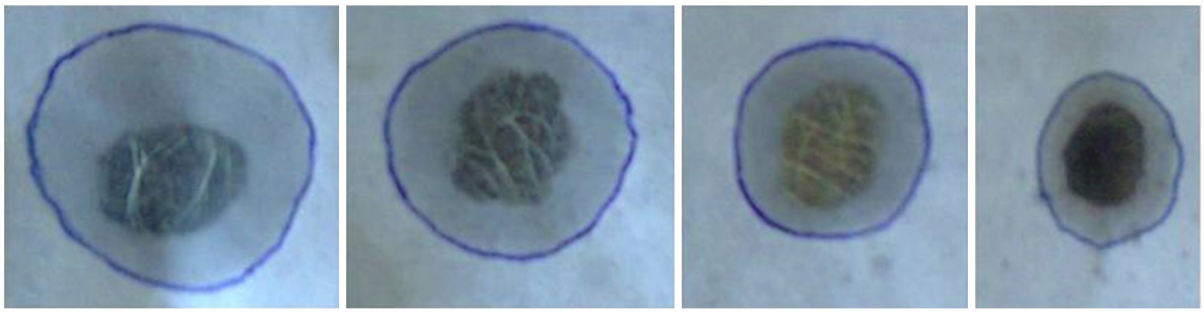

(a) (b) (c) (d)

Figure 7. Images of wetted areas for (a) PVP, (b) PVP-RHA, (c) PVP-RH and (d) PVP-RHC after hydrophilicity test.

actions are strong enough to reduce the accessibility of water molecules to the polar and hydrophile sites/ functional groups in the PVP structure. Also, the degree of hydrophobicity fillers such as carbonious materials, is an important factor for decreasing the composite WVA values.

As seen in Figure 7a, the wetted area is uniform for PVP because it completely dissolves in water and uniformly penetrates in the paper beneath the sample. However, irregular dissolution patterns can be seen in the images of the composites (Figures 7b and 7c) due to their resistance to water absorption. The circles drawn on the surface of the papers after water absorption are the areas where water molecules and the dissolved PVP have penetrated into the paper. While, the dark spots remained in the middle of the circle can be the insoluble solid particles of the bio-fillers. It is worth to mention that, in the wettability investigation of the samples, the order of PVP > PVP-RiHA > PVP-RiH > PVP-RiHC was observed. Undoubtedly, parameters such as the solubility of the additives, their compatibility with the polymer matrix and their effect on the polymer crystallinity and density, play effective roles on the hydrophilicity of the samples.

Effect of incubation time on WVA values

In the practical part of this experiment, 0.01 g of each sample was placed in the WVA chamber and the amount of water vapor absorbed by them was measured at different times of incubation. The results of these investigations are shown in Figure 8. As can be seen, the composites are more hydrophobic than the neat polymer, among which PVP-RHC was the most hydrophobic sample. Regardless of the difference in WVA value for theses polymeric materials, PVP and its composites reached the maximum WVA after about 24 hours (Figure 8).

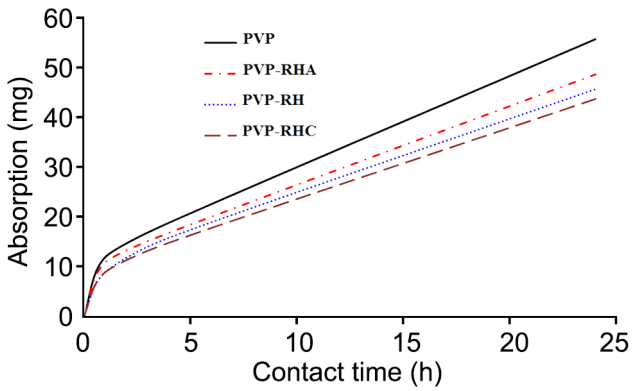

Figure 8. Effect of incubation time on WVA results at ambient temperature and pressure.

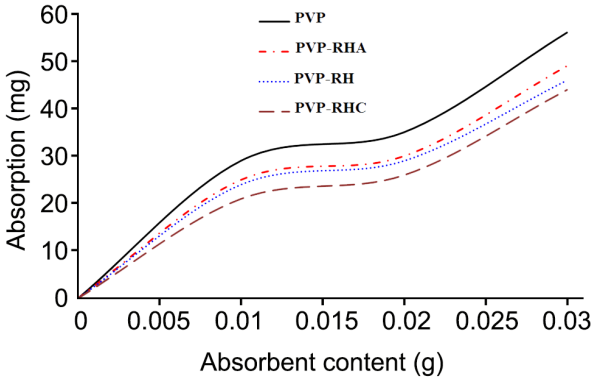

Figure 9. Effect of initial weight of absorbent on WVA results at ambient temperature and pressure after 24 h of incubation.

Effect of initial mass of the absorbent materials on WVA results

As shown in Figure 9, there was an increasing relationship between the content of the absorbed water and the initial weight of the absorbent samples. In addition, it is clear that the WVA values enhanced upon increasing the initial amount of PVP absorbents. In this experiment, the order of PVP>PVP-RiHA>PVP-RiH>PVP-RiHC was observed for the hydrophilicity values of the samples. As a result, this order was also observed for the slope of the curves. In the other word, the pure polymer not only possessed a higher WVA, but also its WVA rate was higher than that of the composites.

CONCLUSIONS

In the current research study, carbonious materials and ash originated from rice husk were obtained through pyrolysis at the temperatures of 300 and 600°C, respectively. The spectroscopic characteristics of PVP and PS composites with RH, RHC and RHA were examined using FT-IR spectroscopy and XRD analysis. The results exhibited a significant difference between the spectra of pure polymers and the corresponding composites spectra. For example, In addition to the decrease in the intensity of FT-IR peaks, there were

significant changes in the wavenumber of some peaks. In the X-ray diffraction results, a decrease in the width and intensity of the peaks was observed, which means an increase in the size of the crystalline areas. Also, new peaks appeared in the XRD spectrums of the composites. These observations indicate the changes in intermolecular bonds, molecular order and crystallinity of the composites as compared to the parent polymers. WVA investigations were conducted for PVP samples, but this property was not studied in the case of PS owing to its negligible hydrophilicity. A significant difference between the hydrophilicity of PVP and composites was observed in the order of PVP>PVP-RiHA>PVP-RiH>PVP-RiHC. Therefore, these additives were observed to be effective on the spectroscopic characteristics of both PVP and PS. Besides, these bio-materials were able to reduce the PVP hydrophilicity. The obtained results show that these bio-additives open a new insight to investigate other characteristics of these bio-composites. Moreover, they open a novel window toward the use of other bio-wastes originating from various plants to reinforce/ modify polyolefins.

CONFLICTS OF INTEREST

The author declares that they have no conflicts of interest.

REFERENCES

1 Asyraf MRM, Ishak MR, Norrrahim MNF, Nurazzi NM, Shazleen SS, Ilyas RA, Rafidah M, Razman MR (2021) Recent advances of thermal properties of sugar palm lignocellulosic fibre reinforced polymer composites. Int J Biol Macromol 193: 1587-1599

2. Mirzajani V, Nazarpour-Fard H, Farhadi K, Ghobadian A (2022) Copper oxide nano-catalyst incorporated TEGDN/NC/DAG propellants: thermal behaviors and kinetics. Propellants Explos Pyrotech 47: p.e202100364

3. Nazarpour-Fard H (2022) Rice husk ash: Economical and high-quality natural-based reinforcing filler for linear low-density and high-density polyethylene. Polym Renew Resour. https://doi.org/10.1177/20412479221128965

4. Nazarpour-Fard H, Rad-Moghadam K, Shirini F, Beheshty MH, Asghari GH (2018) Reinforcement of epoxy resin/carbon fiber composites by carboxylated carbon nanotubes: A dynamic mechanical study. Polimery 63: 254-263

5. Shamsi R, Asghari GH, Mir Mohamad Sadeghi G, Nazarpour-Fard H (2018) The effect of multi-walled carbon nanotube and crosslinking degree on creep–recovery behavior of PET waste originated-polyurethanes and their nanocomposites. Polym Compos 39: E1013-E1024

6. Atta A, Abdelhamied MM, Abdelreheem AM, Althubiti NA (2022) Effects of polyaniline and silver nanoparticles on the structural characteristics and electrical properties of methylcellulose polymeric films. Inorg Chem Commun 135: 109085

7. Nazarpour-Fard H, Behzadi-Pour G, Nasiri-Sarvi M, Esmaili P (2019) PVA-based supercapacitors. Ionics 25: 2951-2963

8. Behzadi-Pour G, Nazarpour-Fard H, Fekri-Aval L, Esmail P (2020) Polyvinylpyridine-based electrodes: sensors and electrochemical applications. Ionics 26: 549-563

9. Behzadi-Pour G, Fekri-Aval L, Nasiri-Sarvi M, Fekri-Aval S, Nazarpour-Fard H (2019) Hydrogen sensors: palladium-based electrode. J Mater Sci Mater 30: 8145-8153

10. Patil S, Bharimalla AK, Mahapatra A, Dhakane-Lad J, Arputharaj A, Kumar M, Raja ASM, Kambli N (2022) Effect of polymer blending on mechanical and barrier properties of starch-polyvinyl alcohol based biodegradable composite films. Food Biosci 44: 101352

11. Putri RM, Sundari CD, Floweri O, Mayangsari TR, Ivansyah AL, Santosa SP, Arcana IM, Iskandar F (2021) PEO/PVA/LiOH solid polymer electrolyte prepared via ultrasound-assisted solution cast method. J Non-Cryst Solids 556: 120549

12. Soni G, Jangir RK (2021) Effect of temperature nano graphite doped polymethylmethacrylate (PMMA) composite flexible thin films prepared by solution casting: Synthesis, optical and electrical properties. Optik 226: 165915

13. Agyei-Tuffour B, Asante JT, Nyankson E, Dodoo-Arhin D, Oteng-Peprah M, Azeko ST, Azeko AS, Oyewole OK, Yaya A (2021) Comparative analyses of rice husk cellulose fiber and kaolin particulate reinforced thermoplastic cassava starch biocomposites using the solution casting technique. Polym Compos 42: 3216-3230
14. Hintermueller D, Prakash R (2022) Comprehensive characterization of solution-cast pristine and reduced graphene oxide composite polyvinylidene fluoride films for sensory applications. Polymers 14: 2546
15. Singh L, Kashyap A, Singh V (2022) Investigating the effect of rGO concentration on rGO-PMMA composites synthesized via solution casting technique. Res Dev Material Sci 17: 1961-1965
16. A Adorna J, G Ventura RL, Dang VD, Doong RA, S Ventura JR (2022) Biodegradable polyhydroxybutyrate/cellulose/calcium carbonate bioplastic composites prepared by heat-assisted solution casting method. J Appl Polym Sci 139: 51645
17. Özuğur Uysal B, Akın Evingür G, Pekcan Ö (2022) Polyacrylamide mediated polyvinyl pyrrolidone composites incorporated with aligned molybdenum disulfide. J Appl Polym Sci 139: 52061
18. Doabi EH, Elmi F, Elmi MM (2022) Facile and novel synthesis of nitrogen doped TiO_2/Acid soluble collagen-polyvinyl pyrrolidone (ASC-PVP) hybrid nanocomposite for rapid and effective photodegradation of naphthalene from water under visible light irradiation. J Photochem Photobiol 425: 113677
19. Dlamini ZW, Vallabhapurapu S, Wu S, Mahule TS, Srivivasan A, Vallabhapurapu VS (2022) Resistive switching memory based on chitosan/polyvinylpyrrolidone blend as active layers. Solid State Commun 345: 114677
20. Elbarbary AM, Bekhit M, El Fadl FIA, Sokary R (2022) Synthesis and characterization of magnetically retrievable Fe_3O_4/polyvinylpyrrolidone/polystyrene nanocomposite catalyst for efficient catalytic oxidation degradation of dyes pollutants. J Inorg Organomet Polym Mater 32: 383-398
21. Zhang YB, Wang HJ, Raza A, Liu C, Yu J, Wang JY (2022) Preparation and evaluation of chitosan/polyvinylpyrrolidone/zein composite hemostatic sponges. Int J Biol Macromol 205: 110-117.
22. Abdulkareem SA, Ighalo JO, Adeniyi AG (2021) Evaluation of the electrical characteristics of recycled iron reinforced polystyrene composites. IJEE 12: 125-130
23. Adeniyi AG, Abdulkareem SA, Ighalo JO, Oladipo-Emmanuel FM, Adeyanju CA (2021) Microstructural and mechanical properties of the plantain fiber/local clay filled hybrid polystyrene composites. Mech Adv Mater Struct 1-11
24. Prucek R, Panáček A, Gajdová Ž, Večeřová R, Kvítek L, Gallo J, Kolář M (2021) Specific detection of Staphylococcus aureus infection and marker for Alzheimer disease by surface enhanced Raman spectroscopy using silver and gold nanoparticle-coated magnetic polystyrene beads. Sci Rep 11: 1-11
25. Ighalo JO, Adeniyi AG, Owolabi OO, Abdulkareem SA (2021) Moisture absorption, thermal and microstructural properties of polymer composites developed from rice husk and polystyrene wastes. Int J Sustain Eng 14: 1049-1058
26. Thomas SK, Parameswaranpillai J, Krishnasamy S, Begum PS, Nandi D, Siengchin S, George JJ, Hameed N, Salim NV, Sienkiewicz N (2021) A comprehensive review on cellulose, chitin, and starch as fillers in natural rubber biocomposites. Carbohydr Polym 2: 100095
27. Arman NSN, Chen RS, Ahmad S (2021) Review of state-of-the-art studies on the water absorption capacity of agricultural fiber-reinforced polymer composites for sustainable construction. Constr Build Mater 302: 124174
28. Kumar J, Kumar V, Singh I, Rakesh PK (2021) Joining behavior of polymeric composites fabricated using agricultural waste as fillers. J Adhes Sci Technol 35: 1652-1663
29. Suhot MA, Hassan MZ, Aziz SAA, Md-Daud MY (2021) Recent progress of rice husk reinforced polymer composites: A review. Polymers 13: 2391
30. You X, Zhou R, Zhu Y, Bu D, Cheng D (2022) Adsorption of dyes methyl violet and malachite green from aqueous solution on multi-step modi-

fied rice husk powder in single and binary systems: characterization, adsorption behavior and physical interpretations. J Hazard Mater 430: 128445

31. Priya AK, Yogeshwaran V, Rajendran S, Hoang TK, Soto-Moscoso M, Ghfar AA, Bathula C (2022) Investigation of mechanism of heavy metals (Cr^{6+}, Pb^{2+} & Zn^{2+}) adsorption from aqueous medium using rice husk ash: kinetic and thermodynamic approach. Chemosphere 286: 131796
32. Riana U, Ramli M, Iqrammullah M, Raharjo Y, Wibisono Y (2022) Development of chitosan/rice husk-based silica composite membranes for biodiesel purification. Membranes 12: 435.
33. Amran M, Fediuk R, Murali G, Vatin N, Karelina M, Ozbakkaloglu T, Krishna RS, Sahoo AK, Das SK, Mishra J (2021) Rice husk ash-based concrete composites: A critical review of their properties and applications. Crystals 11: 168
34. Hanwen H, Lixin M, Aiguo L (2009) The research of polyolefin/rice huck composites. Master's Thesis, School of Materials Science and Engineering, Beijing University of Chemical Technology
35. Nazarpour-Fard H, Rad-Moghadam K, Shirini F, Beheshty MH (2016) Novel improvements in thermal and hydrophobic properties of chitosan reinforced by rice husk ash. Polym Renew Resour 7: 115-133
36. Slobodian P, Pavlínek V, Lengálová A, Sáha P (2009) Polystyrene/multi-wall carbon nanotube composites prepared by suspension polymerization and their electrorheological behavior. Curr Appl Phys 9: 184-188
37. Shirini F, Akbari-Dadamahaleh S, Mohammad-Khah A, Aliakbar AR (2013) Rice husk: A mild, efficient, green and recyclable catalyst for the synthesis of 12-Aryl-8, 9, 10, 12-tetrahydro [a] xanthene-11-ones and quinoxaline derivatives. C R Chim 16: 207-216
38. Shirini F, Mamaghani M, Seddighi M (2013) Sulfonated rice husk ash (RHA-SO_3H): A highly powerful and efficient solid acid catalyst for the chemoselective preparation and deprotection of 1, 1-diacetates. Catal Commun 5: 31-37
39. Seddighi M, Shirini F, Mamaghani M (2015) Brønsted acidic ionic liquid supported on rice husk ash (RHA-[pmim] HSO_4): A highly efficient and reusable catalyst for the synthesis of 1-(benzothiazolylamino) phenylmethyl-2-naphthols. C R Chim 18: 573-580
40. Chen CM, Hsieh TE, Ju MY (2009) Effects of polydispersity index and molecular weight on crystallization kinetics of syndiotactic polystyrene (sPS). J Alloys Compd 480: 658-661
41. Monshi A, Foroughi MR, Monshi MR (2012) Modified Scherrer equation to estimate more accurately nano-crystallite size using XRD. World J Nano Sci Eng 154: 160
42. Shimazu A, Miyazaki T, Ikeda K (2000) Interpretation of d-spacing determined by wide angle X-ray scattering in 6FDA-based polyimide by molecular modeling. J Membr Sci 14: 113-118
43. Wang D, An J, Luo Q, Li X, Li M (2008) A convenient approach to synthesize stable silver nanoparticles and silver/polystyrene nanocomposite particles. J Appl Polym Sci 5: 3038-3046
44. Naim AA, Umar A, Sanagi MM, Basaruddin N (2013) Chemical modification of chitin by grafting with polystyrene usingammonium persulfate initiator. Carbohydr Polym 98: 1618-1623
45. Burcham LJ, Datka J, Wachs IE (1999) In situ vibrational spectroscopy studies of supported niobium oxide catalysts. J Phys Chem B 103: 6015-6024
46. Ajitha B, Reddy YAK, Reddy PS (2014) Biogenic nano-scale silver particles by Tephrosia purpurea leaf extract and their inborn antimicrobial activity. Spectrochim Acta A Mol Biomol Spectrosc 121: 164-172
47. Martins AE, Pereira MS, Jorgetto AO, Martines MA, Silva RI, Saeki MJ, Castro GR (2013) The reactive surface of Castor leaf [Ricinus communis L.] powder as a green adsorbent for the removal of heavy metals from natural river water. Appl Surf Sci 276: 24-30
48. Mireles LK, Wu MR, Saadeh N, Yahia LH, Sacher E (2020) Physicochemical characterization of polyvinyl pyrrolidone: A tale of two polyvinyl pyrrolidones. ACS omega 5: 30461-30467
49. Bharali DJ, Sahoo SK, Mozumdar S, Maitra A (2003) Cross-linked polyvinylpyrrolidone nanoparticles: a potential carrier for hydrophilic

drugs. J Colloid Interface Sci 15: 415-423
50. Crowley KJ, Zografi G (2002) Water vapor absorption into amorphous hydrophobic drug/poly (vinylpyrrolidone) dispersions. J Pharm Sci 91: 2150-2165